Molecular Therapy
Methods & Clinical Development
Original Article

Successful Transduction with AAV Vectors after Selective Depletion of Anti-AAV Antibodies by Immunoadsorption

Alejandro Orlowski,[1] Michael G. Katz,[1] Sarah M. Gubara,[1] Anthony S. Fargnoli,[1] Kenneth M. Fish,[1] and Thomas Weber[1]

[1]Cardiovascular Institute, Graduate School of Biomedical Sciences, Icahn School of Medicine at Mount Sinai, New York City, NY, USA

Gene therapy with adeno-associated virus (AAV)-based vectors shows great promise for the gene therapeutic treatment of a broad array of diseases. In fact, the treatment of genetic diseases with AAV vectors is currently the only *in vivo* gene therapy approach that is approved by the US Food and Drug Administration (FDA). Unfortunately, pre-existing antibodies against AAV severely limit the patient population that can potentially benefit from AAV gene therapy, especially if the vector is delivered by intravenous injection. Here, we demonstrate that we can selectively deplete anti-AAV antibodies by hemapheresis combined with AAV9 particles coupled to Sepharose beads. In rats that underwent hemapheresis and immunoadsorption, luciferase expression was dramatically increased in the hearts and fully restored in the livers of these rats. Importantly, our method can be readily adapted for the use in clinical AAV gene therapy.

INTRODUCTION

Adeno-associated virus (AAV) is a small (25 nm), non-enveloped virus with a single-strand DNA genome.[1] Currently, recombinant AAV vectors (rAAVs) are arguably the most promising DNA delivery vehicle for clinical gene therapy. This is due, in part, to the apparent lack of pathogenicity of the wild-type (WT) virus, the ability to establish long-term transgene expression, at least in non-dividing cells,[2] and the low immunogenicity when compared to other viral vectors.

The great potential of rAAVs for clinical gene therapy is exemplified by the approval by the US Food and Drug Administration (FDA) to treat patients with Leber's congenital amaurosis type 2 (LCA2)[3] and, more recently, patients with spinal muscular atrophy (SMA) with an AAV vector.[3] Moreover, preclinical studies to treat severe hemophilia A and hemophilia B[4,5] with rAAVs will likely result in the approval of these treatments by the FDA in the near future. Unfortunately, there is a high prevalence of pre-existing anti-AAV antibodies in the general population,[6–8] which significantly reduces the patient population that could potentially benefit from AAV gene therapy.

Several strategies have been proposed to overcome this limitation. But, so far, all of them had limited success. Preliminary studies[9] have suggested that one of the most promising strategies might be plasmapheresis. In traditional plasmapheresis to reduce antibodies in immune diseases, blood cells and the plasma components are separated. The plasma is then either replaced by a plasma replacement solution[10] or immunoglobulins are depleted from the plasma by passing the plasma through protein A columns.[10] The immunoglobulin-depleted plasma and the blood cells are then combined and reinfused into the patient. Monteilhet et al.[9] have demonstrated in 10 patients that several rounds of plasmapheresis could lead to a significant reduction in anti-AAV antibodies. It is noteworthy, however, that for instance for AAV2, in only one patient (with an initial neutralizing antibody [NAb] titer of 1/5) all NAbs could be depleted. None of the patients with an initial neutralizing titer of $\geq$10 reached titers that were consistently below 20.

It is needless to say that multiple plasma exchanges of 50% of total plasma volume[9] is not ideal. Moreover, removal of >90% of all immunoglobulins, which would be necessary to drive NAb titers of a patient with an initial titer of $\geq$1/20 to $\leq$2 is not only challenging, but it also comes with its own set of clinical concerns.

Lazaridis et al.[11,12] have designed an improved approach to treat myasthenia gravis by selectively removing autoantibodies with the extracellular domain of the acetylcholinesterase receptor immobilized onto a matrix. A similar approach is used clinically to overcome AB0 incompatibility in renal and liver transplantation by removing antibodies against blood-groups A and B erythrocytes with a column with immobilized carbohydrate antigens.[13,14]

Here, we demonstrate that apheresis and an AAV-Sepharose matrix might be used to overcome the problem of pre-existing anti-AAV antibodies in AAV-based gene therapy.

Received 3 December 2019; accepted 8 January 2020;
https://doi.org/10.1016/j.omtm.2020.01.004.

Correspondence: Thomas Weber, Cardiovascular Institute, Graduate School of Biomedical Sciences, Icahn School of Medicine at Mount Sinai, New York City, NY, USA.
E-mail: thomas.weber@mssm.edu

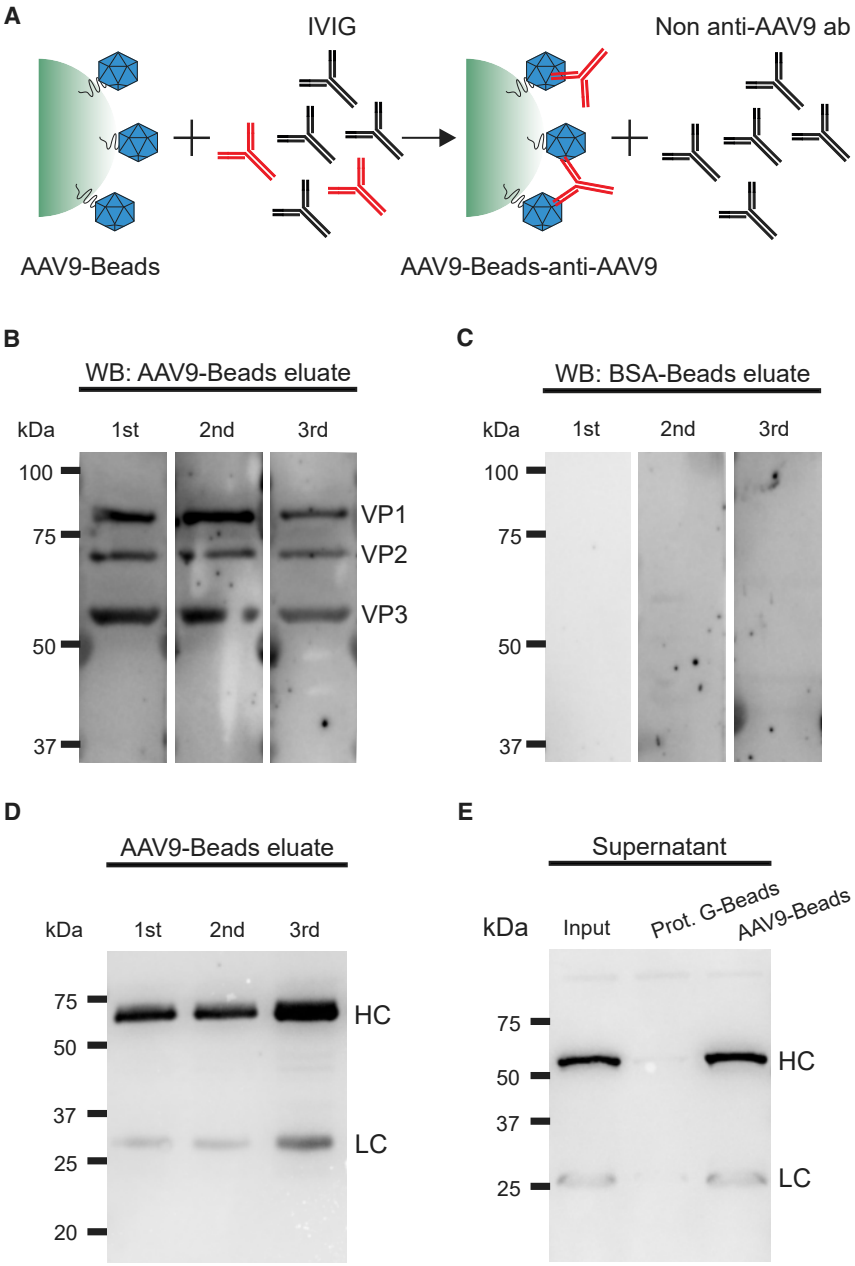

Figure 1. Depletion of Anti-AAV9 Antibodies from an IVIG Solution by Immunoadsorption with AAV9 Sepharose Beads

(A) Schematic depiction of immunoadsorption of anti-AAV9 antibodies. To deplete anti-AAV9 antibodies from a solution with human IVIG (intravenous immunoglobulin), was incubated the solution with Sepharose beads with covalently coupled AAV9 virions (AAV9-beads). (B) After incubation with IVIG solution, the beads were washed with PBS and the anti-AAV antibodies were eluted from the AAV9-beads by incubation with a low pH buffer. After elution of the anti-AAV antibodies, the beads were washed with PBS. The binding/elution procedure was repeated twice. Anti-AAV9 antibodies in the eluates were detected by Western blot with neutralized eluates as a primary antibody. The AAV9 capsid proteins (VP1, VP2, and VP3) were detected with an HRP-anti-human-IgG secondary antibody and ECL. The same matrix was reused three times without evidence of loss of binding capacity. (C) As in (B), but with BSA-beads. (D) Western blot experiment showing the presence of immunoglobulin heavy chain (HC) and light chain (LC) in the AAV9-beads eluates. (E) The total amount of antibodies remained unchanged after the incubation of IVIG with AAV9-beads, but not with protein G-beads.

RESULTS

AAV9-Beads Efficiently Reduced Anti-AAV9 Antibodies in *In Vitro* Experiments

To fabricate the immunoadsorbent matrix (AAV9-beads), we incubated WT-AAV9 with N-hydroxy-succinmide ester (NHS)-activated Sepharose (approximately 1.35×10^{13} viral particles were bound per mL of NHS Sepharose, data not shown). We then tested whether this matrix could bind anti-AAV antibodies present in intravenous immunoglobulin (IVIG). We first incubated an IVIG solution with AAV9-beads or, as a control, bovine serum albumin (BSA)-beads. After washing the beads, we eluted potential anti-AAV9 antibodies by incubating the beads with pH 3.5 buffer. To detect anti-AAV9 antibodies, we performed a Western blot. As can be seen in Figures 1B and 1C, eluate from AAV9-beads, but not BSA-beads, could detect the three AAV9 capsid proteins (VP1, VP2, and VP3). Unlike with classical plasmapheresis (using protein A or protein G columns), the total amount of IgG in the eluate remained unchanged (Figures 1D and 1E), whereas protein G beads completely depleted IgG from the IVIG solution (Figure 1E). Moreover, we were able to re-use the matrix at least three times without any evidence of loss of binding capability as demonstrated by an ELISA (Figure 2). To determine the maximum binding capacity of the matrix, we incubated increasing amounts of IVIG with the AAV9-beads (Figure 3). The beads were then washed and the bound antibodies eluted with low pH buffer. The total amount of bound antibodies was calculated by ELISA and yielded a maximum capacity of ~120 mg of IVIG/mL of AAV9-beads.

As expected, when we incubated an IVIG solution with AAV9-beads, the addition of the supernatant to cells did not inhibit AAV9 transduction (Figure 4B). This was not the case when BSA beads were used (Figure 4B). Furthermore, neutralized supernatant of IVIG incubated with AAV9-beads, but not BSA-beads, strongly inhibited HEK293T transduction (Figure 4C).

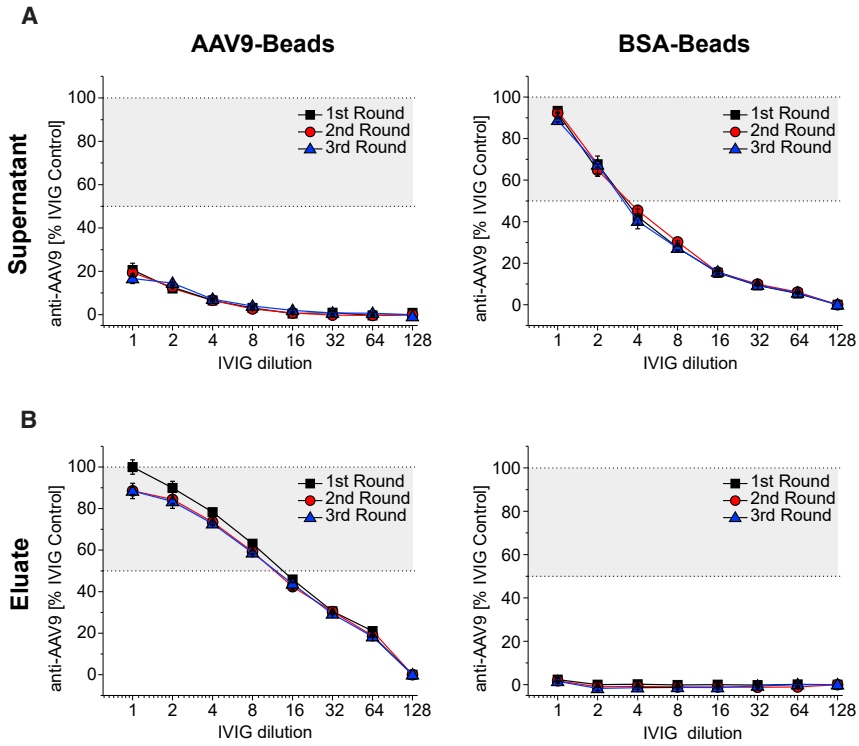

Figure 2. Analysis of Total Anti-AAV9 Antibody Titers in the Supernatants and Eluates of the Experiments Described in Figure 1

(A) Total amounts of anti-AAV9 antibodies in the supernatants (Figure 1) were determined by ELISA. (B) Total amounts of anti-AAV9 antibodies in the eluates (Figure 1) were determined by ELISA. The data are depicted as the mean ± standard error (n = 3).

Confirming our ELISA data (Figure 2), the beads could be used at least three times to deplete NAbs present in IVIG (Figure 4).

Reduction of Anti-AAV9 Antibodies in Human Samples

To demonstrate that AAV9-beads are also able to deplete anti-AAV antibodies from individual human sera, we screened human sera samples and selected 5 sera with NAb titers ranging from 1/4 to 1/128. After a single round of incubation of the sera with AAV9-beads, we dramatically decreased both the NAb titers, as well as the total anti-AAV9 antibodies (Figure 5; Table S1). The modest reduction of NAbs and total-anti-AAV antibodies in human serum 5 (NAb titer of 1/128) was likely due to the fact that this serum exceeded the binding capacity of the beads. Interestingly, in the experiments with human serum 1 (NAb titer of 1/4), transduction at a serum dilution of 1/2 was not fully restored. Similarly, the depletion of immunoglobulins of human serum 1 was incomplete. Because both neutralizing and non-neutralizing immunoglobulins bind to AAV9 beads, the easiest explanation for the lack of complete restoration of transduction by incubation with AAV9 beads is that the binding of non-neutralizing immunoglobulins prevented the complete depletion of neutralizing factors. In fact, our data—compare our NAb results with our ELISA results (e.g., human serum 4; NAb titer 1/32)—and data by others[15] demonstrate that the correlation of ELISA and NAb results depends on the specific human serum analyzed. The presence of neutralizing factors against AAV9 in the general population is low. In fact, among the 10 sera tested for (Figure 5), only 5 were positive for neutralizing factors in our NAb assay. Nonetheless, even in the absence of depletion experiments of multiple low NAb titer samples, taken together, our *in vitro* experiments conclusively demonstrate that AAV9-beads can deplete NAbs and potential other neutralizing factors from human sera—even with a single round of incubation with AAV9 beads.

Similarly to AAV9, incubation of IVIG with AAV2 coupled to beads was able to deplete neutralizing antibodies/factors from IVIG solutions (Figure S1). Thus, our approach is likely applicable to many AAV serotypes and variants.

It has recently been reported that AAV5 has an unusual immune profile.[16–18] For instance, a recent publication suggests that non-human primates with NAb titers of an average of >5,000 show only a 2.9-fold reduction in transduction compared to animals that are negative for NAbs.[18] Unfortunately, a detailed description of the NAb assay is not provided by Ferreira and colleagues.[18] However, a thorough investigation of the literature cited in Salas et al.[18] (and of relevant articles that have been cited in articles referenced in their publication[16,17]) suggests that in their NAb assay, the number of vg-containing particles per μL serum is $\sim 3.8 \times 10^5$.

In our NAb assay, on the other hand, we used 1×10^7 vg-containing particles/μL serum. Put differently, had we used the same number of vg-containing particles/μL serum that was apparently used by Salas et al.,[16–18] our NAb titers of 1/4 and 1/128 would translate to NAb titers of 106 and 3,368, respectively. Clearly, the AAV gene therapy community—at the very least—needs to modify the way of reporting of neutralizing AAV transduction capacities of sera to be able to compare NAb titers among different articles.

This is critical since, for the reasons just described, it is currently difficult to judge whether systemically delivered AAV5 is truly less sensitive to anti-AAV5 antibodies when compared to the sensitivity of other serotypes to antibodies against the serotype administered (e.g., Salas et al.[18] and Falese et al.)[15]

In Vivo Immunoadsorption of Anti-AAV Antibodies

Because of the small blood volume of rats, plasmapheresis is challenging. However, Lazaridis et al.[11] have demonstrated that whole-blood apheresis can be performed in rats after an implantation of a femoral vein catheter. To test whether we could use hemapheresis

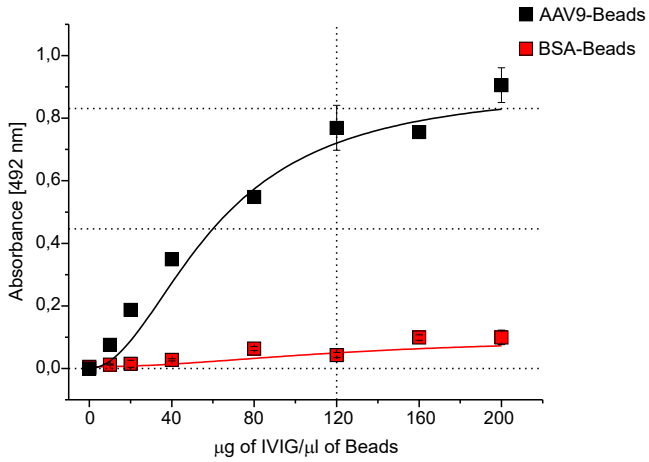

Figure 3. Binding Capacity for Anti-AAV9 Antibodies

50 µL AAV9-beads or BSA-beads were incubated with increasing concentrations of IVIG. The coupled antibodies were eluted and the amount of anti-AAV9 antibody bound was determined by ELISA. The data are depicted as the mean ± standard error (n = 3).

and an AAV matrix to deplete anti-AAV antibodies from the blood of rats, we used a similar approach. To gain blood access, we implanted a catheter into the jugular vein of the rats.

Initially, we attempted to use active immunization to obtain a group of animals with an appropriate range of NAb titers. Unfortunately, the variability in neutralizing titers (using different amounts of virus as antigen) was too unpredictable to be practical (and humane) for our experiments. Hence, we decided to use a passive immunization method for the experiments described here. A single intradermal injection of serum from a rat with a very high anti-AAV titer was used to passively immunize the rats. This allowed us to predict with reasonable accuracy the neutralizing titer after 24 h, which (without immunoadsorption) stayed constant for at least 3 days (Figure S2).

After a single round of hemapheresis, we observed a rapid rebound of antibodies from the interstitial/lymphatic compartment. In fact, 3 h after hemapheresis the concentration of neutralizing antibodies/factors exceeded 60% pre-hemapheresis levels, and at 24 h the levels were equal to the antibody/neutralizing fact levels before the first hemapheresis session (Figure S3A). As has been shown in by Kotchey et al.[19] in mice, the blood clearance of AAV9 was slow. In our experiments in rats, even 24 h after virus injection the concentration of AAV9 was essentially unchanged when compared to levels 2 h after virus injection (Figure S3B). In order to mitigate the effect of antibody rebound on transduction, we performed 3 consecutive immunoadsorption sessions, 1 h apart. In each session, approximately 1 blood volume was drawn, incubated with beads, and then re-infused into the rat (for details see Materials and Methods). Blood samples were taken before and after each session. Figure 6 shows the results of NAb assays and ELISA from sera samples from 2 representative rats with initial NAb titers of 1/8 and 1/16, respectively. In contrast to their base line titers, none of the rats had any NAbs in their blood (Figure 6B) and their total anti-AAV antibodies were dramatically reduced (Figure 6C).

Immediately after the last session, the rats were tail vein injected with AAV9-luciferase (8×10^{12} vg/kg). Control rats with corresponding NAb titers were injected with an equal amount of AAV9-luciferase.

21 days after viral injection (Figure 7A), we performed *in vivo* imaging to evaluate viral transduction. In sharp contrast to control rats, rats whose NAbs were depleted with immunoadsorption showed significant expression of luciferase in the liver/heart and skeletal muscle area. The data for pairs of rats with NAb titers of 1/8 and 1/16 are shown in Figures 7B and 7C, respectively. The data for other rats are shown in Figure S5.

At the time of sacrifice (day 28, Figure 7A), the heart, liver, and skeletal muscle (quadriceps) of the rats were collected and luciferase expression was accurately quantified *in vitro*. In all rats that were passively immunized, but were not subjected to immunoadsorption, luciferase expression was reduced >50,000-fold when compared to naive rats (Figures 7B and 7C). In sharp contrast, luciferase expression in the heart and liver in rats that had undergone immunoadsorption was dramatically increased (Figures 7B and 7C). In fact, expression in the livers was equal to expression levels in the livers of naive rats. On the other hand, while there was a clear trend toward increased transduction of muscle of rats that had undergone immunoadsorption, the increase was not statistically significant (Figure 7).

DISCUSSION

The administration of AAV as a gene therapy vector is currently a resource used in the clinic for the treatment of LCA2[3] and patients with SMA.[3] Additionally, recent promising data from hemophilia clinical trials corroborate the enormous potential of this vector showing that AAV can efficiently transduce liver when it is injected systemically.

The humoral immune response against AAV due to exposure to the WT virus is a significant obstacle for AAV-based gene therapy, especially if the vector is injected systemically. The presence of even very low titer of NAbs can severely reduce or even block the transgene delivery into the target organ. For this reason, the current approach to address this problem is to exclude seropositive patients from these therapies. Moreover, for the successful treatment of certain diseases, re-administration of the virus will be necessary. In these cases, although the patient was seronegative at the time of the first AAV vector administration, the humoral immune response induced by the initial vector administration will prevent the successful transduction upon repeat vector delivery. A number of different strategies have been proposed to circumvent this limitation of AAV-based gene therapy. These approaches include plasmapheresis, addition of empty

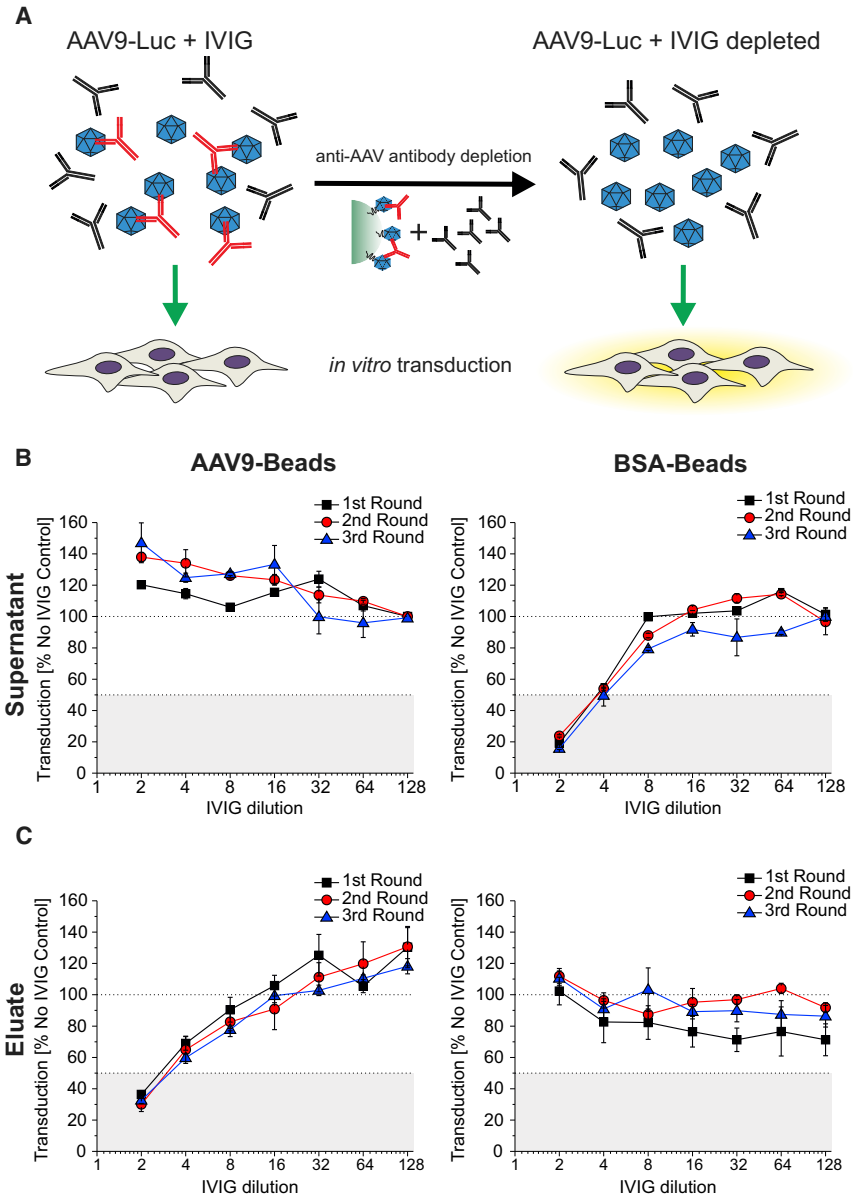

Figure 4. IVIG but Not Supernatants of IVIG Solutions Incubated with AAV9-Beads Inhibit Transduction of HEK293T Cells with AAV9-Luc

(A) Anti-AAV9 antibodies were depleted from human IVIG solutions by incubation with AAV9-beads (BSA-beads served as a control). The same beads were used for three rounds of depletion (see Figure 1 and text). (B) 2-fold dilutions of the supernatants of the IVIG solutions with AAV9-beads or BSA-beads were used to detect transduction of HEK293T cells by an AAV9 vector-encoding luciferase (AAV9-Luc). For details, see Materials and Methods section. (C) After the incubation with the AAV9-beads or BSA-beads, bound anti-AAV9 antibodies were eluted with low pH buffer. Neutralized supernatants were then used to detect the presence of neutralizing antibodies against AAV9 as described in (B). The transduction efficiency is expressed as percent of no-serum control samples. The data are depicted as the mean ± standard error (n = 3).

capsid-decoys, capsid engineering, the administration of immunosuppressants, and direct injection of the AAV in the target tissue.[20–23]

In this report, we describe the preparation of an immunoadsorbent matrix for anti-AAV9 antibodies, which can be used for the elimination of anti-AAV9 antibodies in IVIG solution or in human serum. We also show that the reduction of antibodies was specific for antibodies against AAV9, while no significant reduction in total antibodies was observed. Of note, using an immunoadsorbent matrix for AAV2 antibodies, we were also able to deplete anti-AAV2 antibodies from IVIG solutions (Figure S1), indicating that our approach is likely broadly applicable to multiple AAV serotypes and variants.

Moreover, we show that the combination of immunoadsorption and hemapheresis efficiently reduces the presence of neutralizing antibodies against AAV9 in rats that were passively immunized with anti-AAV9 serum. Due to the significant antibody reservoir in the interstitial fluid and the ensuing "rebound effect" (Figure S3), we performed 3 rounds of immunoadsorption, each 1 h apart. Surprisingly, we didn't observe any differences in neutralizing antibodies in sera collected between the sessions. Interestingly, in contrast to our results obtained with a NAb assay, we saw a clear decline in total anti-AAV antibody levels, as measured by ELISA experiments, after each immunoadsorption session.

The transduction of all organs tested in rats with initial neutralizing titers of 1/8 or 1/16 was completely inhibited by the NAbs (Figure 7). However, when AAV9-Luc was injected after the last session of the hemapheresis and immunoadsorption, the transduction levels in the heart dramatically increased and luciferase expression was completely restored in the liver (Figure 7). Although there was a clear trend toward increased luciferase expression in muscle, the increase was not statistically significant (Figure 7).

As we have shown in Figure S4A, NAb titers recovered by more than 50% 3 h after transduction and were fully restored at 24 h. In contrast to most organs, blood vessels in the liver have extraordinarily large fenestrations: ~280 nm.[24] This means that the virus (with a diameter of ~25 nm) that escapes into the liver likely does so during "first passage." Because of this, this virus is not subject to an anti-AAV antibody rebound effect (Figure S3), which likely explains the complete restoration of luciferase expression (Figure 7).

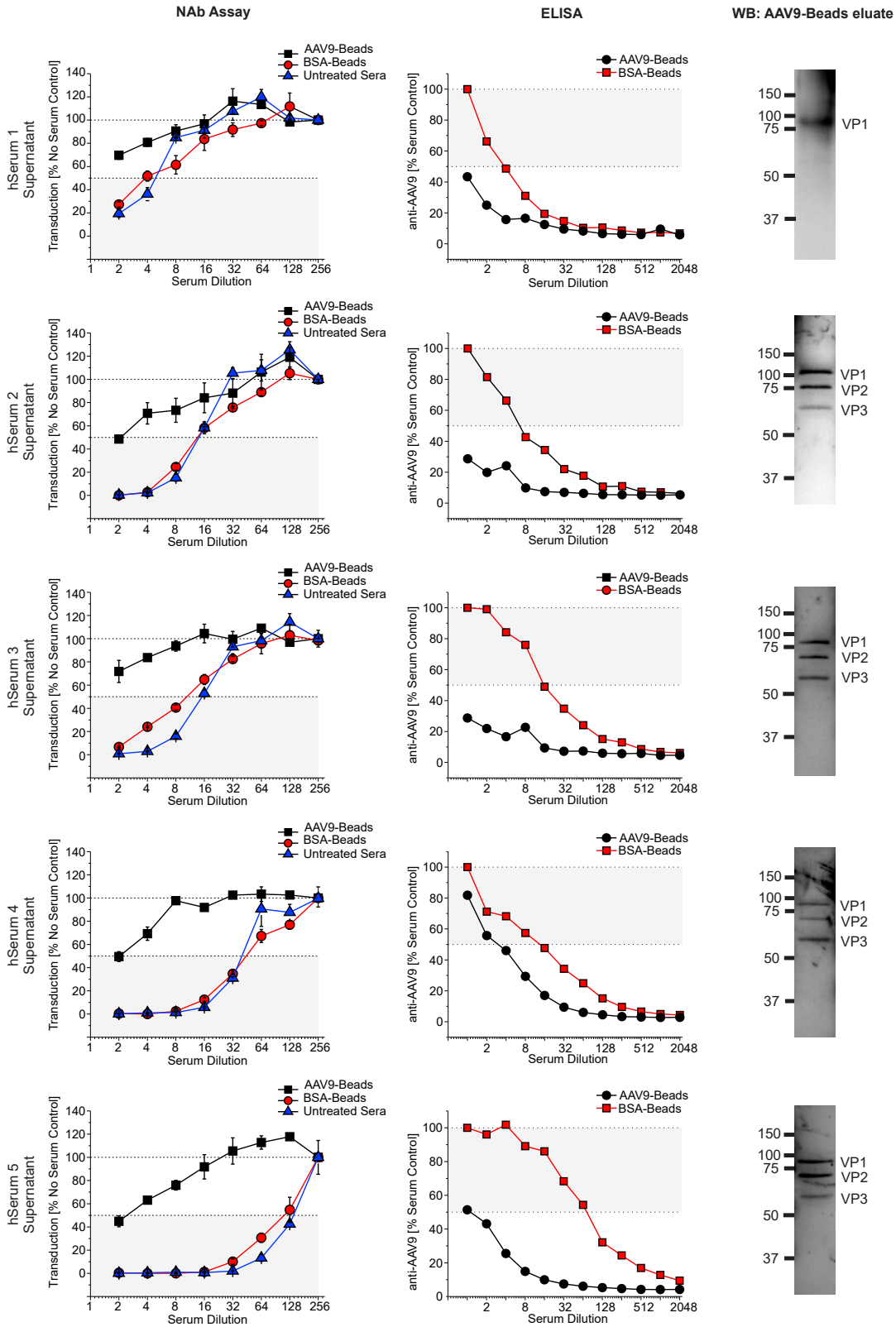

(legend on next page)

In contrast to the liver, the vasculature in skeletal muscle and in the heart has fenestrations of only ~5 nm.[24] These small fenestra almost certainly limit the efficacy and kinetics of escape of AAV from the vasculature. In non-immunized animals, the titers of AAV9 in the blood do not decline significantly for at least up to 3 days (Figure S3B). This should allow the continued escape from vessels with small fenestrations and the potential transduction of skeletal myocytes or cardiomyocytes.

In immunized animals that underwent hemapheresis, NAb titers rapidly rebound (~60% at 3 h). As a result, AAV9 particles in the blood stream will be rapidly neutralized and can no longer transduce skeletal myocytes or cardiomyocytes, even after escape from the vasculature. This likely explains the more modest enhancement of transduction of the heart and the limited, though not statistically significant, increase in the transduction of muscle (Figure 7). The easiest explanation for the more pronounced enhancement of transduction in the heart, when compared to skeletal muscle, in animals that underwent hemapheresis, is the ~10-fold higher capillary density in the heart when compared to skeletal muscle.[25]

Because the virus stays in the blood circulation for a long time (Figure S3B), it is likely that transduction in the heart, and especially in muscle, could be enhanced further by repeated immunoadsorption over a number of weeks. Unfortunately, all our attempts to do so failed because the rats managed to remove their catheters (despite being housed in individual cages).

In conclusion, here we demonstrate, for the first time, that antibodies against AAV can be selectively depleted from the blood of animals by using hemapheresis and AAV-beads. To our knowledge, we report the first *in vivo* depletion of anti-AAV specific antibodies ever published. Significantly, our immunoadsorption technique allows the successful transduction of the heart and liver (and to a lesser extent muscle) of animals that without immunoadsorption wouldn't show any transduction as a result of NAbs.

Most importantly, we expect that our approach will be readily translatable into the clinic and that it will allow the treatment of a much larger number of potential patients that could benefit from gene therapy with AAV vectors.

MATERIALS AND METHODS

Animal Procedures

All procedures involving the handling of animals were approved by the Institutional Animal Care and Use Committee (IACUC) of the Icahn School at Mount Sinai and adhered with the Guide for the Care and Use of Laboratory Animals published by the National Institutes of Health. All animals were provided with nesting material, had *ad libitum* access to food and water, and were housed in a facility with a 12 h/12 h light/dark cycle.

In Vitro Immunoadsorption

WT-AAV9 or WT-AAV2 was coupled to NHS-Activated Sepharose 4 Fast Flow (cat. no: 17090601, GE Healthcare), according to the manufacturer's instructions. NHS-activated Sepharose (beads) was washed with 15 gel volumes of cold 1 mM hydrochloric acid to remove the isopropanol in the storage solution. The pH of the WT-AAV solution was adjusted to pH 8.3, added to the beads in PBS, and incubated overnight at 4°C with mechanical rotation. Approximately 1×10^{14} WT-AAV9 particles were incubated with 25 mL of NHS-Sepharose. For WT-AAV2, approximately 1×10^{13} particles were incubated with 2 mL of NHS-Sepharose. Sepharose beads coupled with 10 mg of albumin (BSA) were used as a control. After the coupling reaction, the non-reacted groups of the beads were blocked with 0.1 M Tris hydrochloride (pH 8.5) for 1 h with agitation at room temperature. The beads were then washed consecutively with buffer A (0.1 M acetate buffer, 0.5 M NaCl, pH 4) and buffer B (0.1 M Tris hydrochloride buffer, pH 8). The beads were washed 5 times. Each time, 3 volumes of washing solutions were used. The beads were kept at 4°C in PBS solution. The coupling efficiency was determined with SDS-PAGE followed by Coomassie staining to visualize the AAV capsid proteins or BSA before and after the incubation with NHS-activated Sepharose.

For the *in vitro* experiments, 200 μL of the AAV-beads or BSA-beads were mixed with 400 μL of dilutions of human serum or IVIG and incubated for 20 min at room temperature. For the elution of immunoglobulins bound to the beads, the beads were first washed with 5 times with 10 bead volumes of PBS. Then 0.5 bead volume of 0.1 mM citric pH 3.5 was added followed by incubation for 5 min at room temperature. After pelleting the beads, the supernatant was immediately neutralized by adding 0.1 volume of 1 M Tris hydrochloric acid, pH 8.

In Vivo Hemapheresis and Immunoadsorption

Catheter Implantation

The rat was placed in a chamber exposed to 4% isoflurane and oxygen (1 L/min) until the rat was anesthetized. The rat was intubated with a 16G catheter and connected to a ventilator set to 70 breaths/min with 2%–2.5% isoflurane. The surgical areas (back and neck) were shaved and then cleaned with 10% povidone-iodine solution followed by 70% ethanol. The animal was placed on top of sterile drapes. The first incision was made on the rat's back, in the center just below the shoulders. Using a long hemostat, a channel was made for the catheter to the right side of the neck. Next, the animal was flipped over and a small incision was made on the right lateral side of the neck, above the subclavian junction. Once the jugular vein was exposed, 3-0 prolene suture was used to prevent bleeding. The catheter was flushed with 1%

Figure 5. Depletion of Anti-AAV Antibodies in Human Serum Samples by Immunoadsorption

In vitro depletion of anti-AAV9 antibodies from 5 human sera with neutralizing titers of 1/4, 1/8, 1/16, 1/32, and 1/128, respectively. Incubation and elution was performed as described in Figure 1. Neutralizing antibody titers were determined as in Figure 2, and total anti-AAV9 antibodies amounts were quantified by ELISA. The data are depicted as the mean ± standard error (n = 3). Western blot was used to confirm that the antibodies eluted from AAV9-beads were specific for AAV9 capsid proteins (see also Table S1).

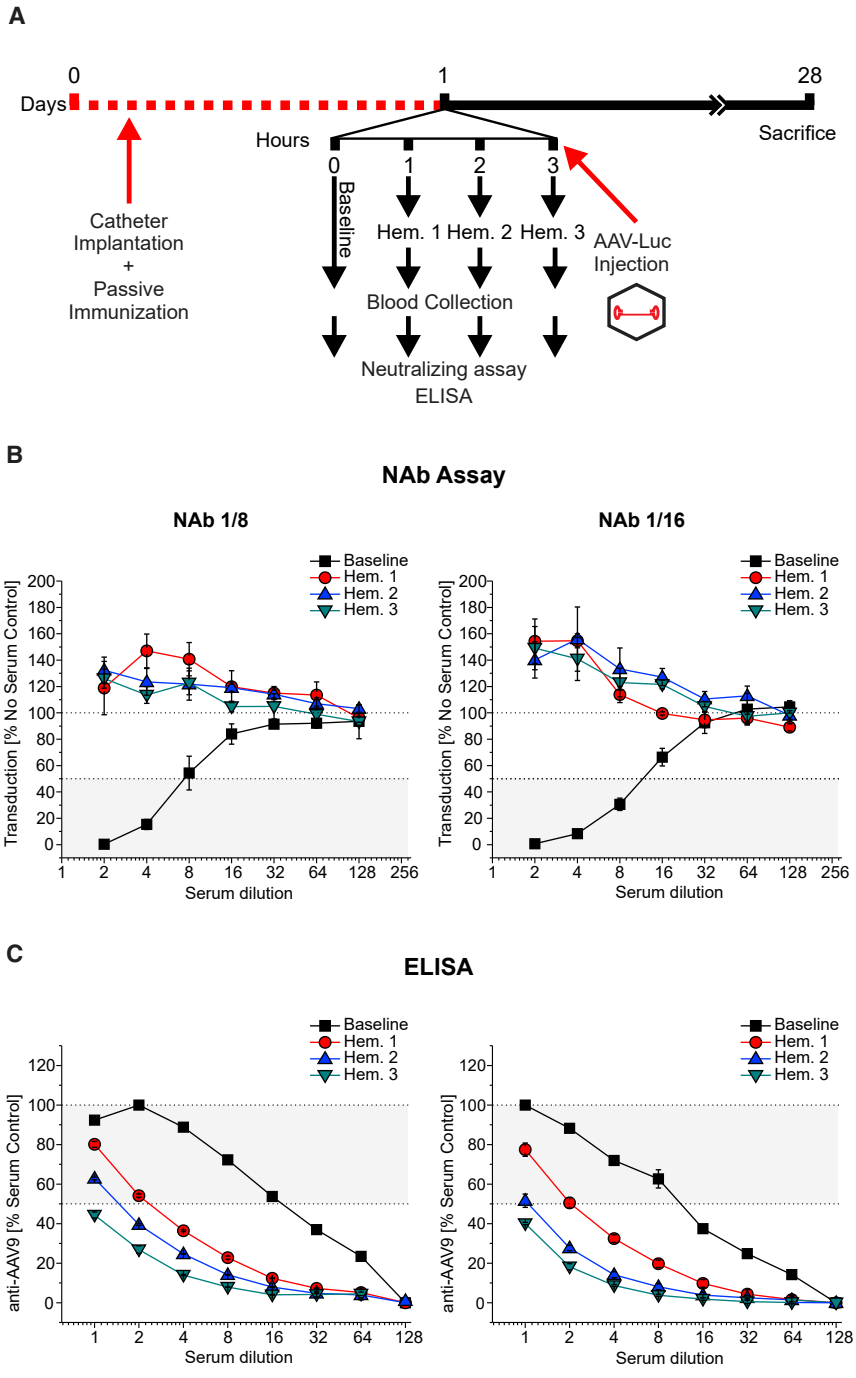

Figure 6. Hemapheresis and Immunoadsorption with AAV9 Beads Depletes Anti-AAV9 Antibodies from the Blood of Passively Immunized Rats

(A) Experimental scheme of the depletion protocol. At day 0, catheters were implanted into the jugular vein of rats that were passively immunized with anti-AAV9 rat serum. On day 1, rats underwent three rounds of hemapheresis and immunoadsorption with AAV9 beads. Blood was drawn immediately before the first hemapheresis session (baseline) and immediately after each round of hemapheresis. Immediately after the last hemapheresis session, 8×10^{12} vg/kg of AAV9-Luc was injected. (B) Sera from the blood samples described in (A) were used for neutralization assays (see Figure 2). (C) Total anti AAV9 antibodies were determined by ELISA (for details, see Materials and Methods section). The data are expressed as the percentage of total-anti AAV9 antibodies at baseline.

heparin solution. The catheter was then inserted into the neck incision and threaded through the channel until the end of the catheter emerged from the back incision. A 1 mL syringe with 1% heparin was placed on that end. The other end of the catheter was marked with the distance from the incision to the inferior vena cava. Using small vascular scissors, the vein was cut slightly above the subclavian junction (to prevent disrupting the venous circulation to the upper body). The previously placed control suture was kept tight to avoid bleeding. Using small, fine vascular forceps, the marked end of the catheter was inserted into the jugular vein up to the mark on the catheter. Another suture was tied to secure the catheter into the jugular vein. We made sure that the catheter worked by aspirating blood from the syringe. When blood easily made its way through the catheter and into the syringe, the catheter was flushed with 1% heparin-saline and secured with Vetbond. The incision on the neck was closed. The animal was then turned over. Once we confirmed the blood was flowing through the catheter easily, the catheter was flushed and secured with Vetbond and the incision on the back was closed. We cut the extra length of the catheter so that only 2 inches were exposed. To prevent clotting, we filled the catheter with 0.1–0.2 mL of heparin-glycerin mixture (500 IU heparin/mL in 50% glycerin; HGS-10, SAI Infusion Technologies) solution and sealed by inserting a stainless steel tip. The catheter was secured to the rat's back in a loop using discrete sutures and Vetbond so that that the rat could not remove it. After the surgery, we turned off the isoflurane but continued to administer oxygen to the animal via the endotracheal tube. When the animal started making spontaneous breathing motions and neck movements and responded to physical stimuli, we extubated the rat and disconnected the ventilator. The animal was then placed (and kept) in a separate cage to recover.

Hemapheresis and Immunoadsorption

For *in vivo* experiments, immunoadsorption columns were constructed as described previously.[11] Briefly, a nylon net filter 40 μm

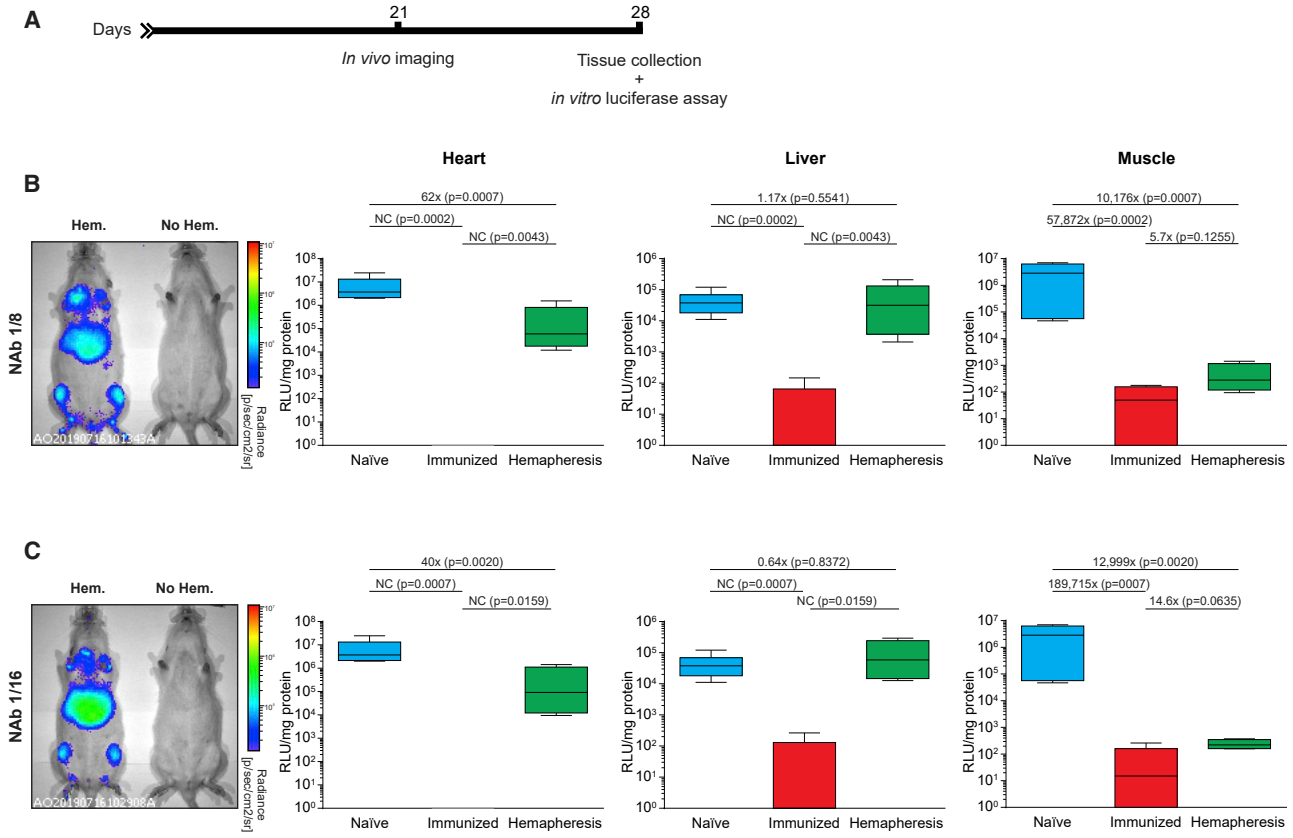

Figure 7. Depletion of Anti-AAV9 Antibodies by Hemapheresis and Immunoadsorption from the Blood of Passively Immunized Rats Allows the Successful *In Vivo* Transduction with AAV9-Luc

(A) Timeline of experiment. (B) Expression of luciferase determined by *in vivo* imaging (day 21; left) and luciferase expression measured *in vitro* (day 28; right) in tissue of the heart, liver, and skeletal muscle harvested at the day of sacrifice. The average of background luminescence in tissues of uninjected rats (n = 4) was subtracted from the values obtained in animals that were injected with AAV-Luc. The neutralizing titer of immunized animals or of immunized animals before hemapheresis and immunoadsorption was 1/8. Naive animals (n = 10), immunized (n = 6), immunized plus hemapheresis and immunoadsorption (n = 5). NC, not calculable because the values of immunized rats were below zero RLU/mg (relative luciferase units/mg protein) (C) As in (B) but the neutralizing titer of immunized animals or of immunized animals before hemapheresis and immunoadsorption was 1/16. Naive animals (n = 10), immunized (n = 5), and immunized plus hemapheresis and immunoadsorption (n = 5). Boxes correspond to upper and lower quartiles, the horizontal line represents the median, and the whiskers mark the minimum and maximum values. The fold differences in expression levels and p values among the groups are indicated. Statistical analysis was done by Mann-Whitney test. See also Figure S4 and for raw data see Table S2.

pore diameter (Millipore) was glued to the bottom of a 5 mL syringe close to the needle adaptor. The pore of the filter allowed the passage of blood cells but not the beads. For the hemapheresis, rats were anesthetized with 4% of isoflurane and oxygen and attached to the ventilator via a nose cone. A syringe containing 2 mL of AAV9-beads (see above) was attached to the catheter. 2 mL of blood was drawn into the syringe filled with AAV9-beads and immediately returned to the circulation. This procedure was repeated 10 times in three different sessions, each 1 h apart. Before and after each session, blood samples were collected and the sera were used for neutralizing antibody assay and ELISA experiments. Immediately after the last hemapheresis/immunoadsorption session, 8×10^{12} vg/kg of AAV9-Luc were injected into the tail vein. After the incubation with the serum solution, the beads were washed with 2 volumes of PBS 5 times and incubated with 0.5 volume of citric acid 0.1 mM solution pH 3.5 for 5 min. After the incubation, the beads were pelleted and the supernatant was immediately neutralized by adding 0.1 volume of Tris hydrochloride 1 M pH 8. The beads were washed again with 2 volumes of PBS 5 times and reused in another round of hemapheresis. The beads could be regenerated at least 3 times.

Preparation of WT-AAV and Recombinant AAV-Luc

Recombinant AAV9-Luc or AAV2-Luc was produced essentially as previously described.[20] The day before transfection, triple flasks (total surface area 500 cm^2) were each seeded with one confluent 15 cm dish of HEK293T/17 (CRL-11268, ATCC) cells and incubated overnight at 37°C and 5% CO_2. Once 90% confluence was reached, transfection was performed by adding the following to 20 mL of room temperature DMEM: 50 μg of *cis*-plasmid (firefly luciferase from pCMV-GL3), 150 μg of pDG9 or pDG2 (briefly vortex), and 250 μL of PEI-max (Polysciences) solution (pH 4.5). For WT-AAV9 and WT-AAV2 production, 66 μg of pAV9 or pAV2 plasmid and 133 μg of pHELPER

were used. The solution was vortexed for 10 s and incubated at room temperature for 15 min. The transfection mix was then added to 90 mL of pre-warmed DMEM containing 2% FBS and mixed by swirling. The medium from the triple flasks was removed and replaced with the transfection mixture. After 3 days of growth, the cells were harvested by vigorous tapping of the flask, transferred to a sterile container, and pelleted by centrifugation. The supernatant was kept for downstream processing. The cell pellet was resuspended in 5 mL of lysis buffer (150 mM of NaCl, 50 mM of Tris hydrochloride, pH 8.5, and 2 mM of $MgCl_2$), and freeze-thawed three times at −80°C and 37°C with brief vortexing after each thaw cycle. Non-encapsidated DNA and contaminating RNA was then digested by adding 2 μL (10 IU/μL) of Pierce Universal Nuclease (cat. no.: 88700, Thermo Fisher Scientific) followed by incubation for 30 min at room temperature. The crude cell lysate was centrifuged to pellet debris, and the supernatant was reserved for iodixanol (cat. no.: D1556, Sigma-Aldrich) gradient ultracentrifugation. Virus from the cell culture supernatant was precipitated by the addition of 31.3 g of ammonium sulfate per 100 mL of supernatant followed by incubation on ice for at least 30 min. The precipitate was pelleted via centrifugation, resuspended in 5 mL of lysis buffer, and then combined with the cell pellet supernatant for iodixanol gradient ultracentrifugation. Samples for ultracentrifugation were prepared in 32.4 mL of polypropylene Optiseal tubes (Beckman Coulter). Viral lysates were loaded on top of discontinuous iodixanol gradients composed of 4 mL of 60% iodixanol, 4 mL of 40%, 4.9 mL of 25%, and 7.3 mL of 17% (with 1 M sodium chloride). The gradients were centrifuged at 350,333 × *g* (avg) for 60 min at 18°C in a Beckman type 70 Ti fixed angle rotor. Fractions (1.25 mL) were collected from the bottom of the tube and kept for virus titration. Peak fractions were dialyzed in lactated Ringer's solution (Baxter International), filtered through a 0.22 μm pore filter (Merck Millipore), and stored at −80°C.

Neutralization Assay

293T/17 cells (ATCC CRL-11268) were maintained in DMEM supplemented with 10% FBS and 1% penicillin/streptomycin at 37°C and 5% CO_2. 1×10^4 cells/well in medium with penicillin/streptomycin were seeded into 96 well-plates (cat. no.: 08-772-2C; Thermo Fisher Scientific) and incubated overnight. The following morning, 2-fold serial dilutions of the sera, IVIG, or eluate solutions were prepared in DMEM in a separate 96-well plate. The concentrations ranged from 40 μL undiluted solution to 1/64 diluted solution. Wells with the same volume of DMEM served as no-serum controls. 2×10^8/well viral genomes of AAV-Luc in 40 μL of DMEM were added to the sera samples or the DMEM control wells (in triplicate), incubated at 37°C for 30 min, and then added to the 293T cells. 24 h later, the transduction efficiency was analyzed by quantifying luciferase activity. The percentage of inhibition was calculated relative to positive, no-anti-AAV (DMEM) control samples. The highest dilution with <50% transduction efficiency was defined as the NAb titer.

Luciferase Assay

The 293T/17 cells for the luciferase assay analysis were lysed by adding an equal amount of 2× lysis buffer (25 mM Tris hydrochloride pH 8, 2 mM DTT, 2 mM EDTA, 10% glycerol, and 1% Triton X-100) followed by an incubation at room temperature on a shaker for 10 min. 20 μL of the cell lysates were added to a black 96-well FluoroNunc plate (cat. no. 12-565-275; Thermo Fisher Scientific). For rat tissues, approximately 25 mg of pulverized tissue from each organ was mixed with 500 μL of lysis buffer, vortexed for 15 s, and then agitated at room temperature for 15 min. The samples were subjected to three cycles of freeze thawing at −80°C to 37°C with brief vortexing after each thaw cycle and incubated overnight at 4°C with agitation. The next day, samples were centrifuged at 12,000 × *g* for 3 min to pellet debris. Protein concentrations were determined by a BCA (bicinchoninic acid) protein assay (cat. no.: 23227; Pierce, Thermo Fisher Scientific) according to the manufacturer's instructions. The luciferase reaction was initiated by the addition of 100 μL of the reaction buffer (25 mM Tricine hydrochloride pH 7.8, 5 mM magnesium sulfate, 0.5 mM EDTA, pH 8.0, 3.3 mM DTT, 0.5 mM ATP pH ~7–8 [A26209; Sigma-Aldrich], 1 mg/mL BSA, 0.05 mg/mL D-luciferin [cat. no.: LUCK-100, Gold Biotechnology], 0.05 mM co-enzyme A [cat. no.: 13787, United States Biological], and was read in a luminescence counter (Microbeta Trilux 1450 LSC Luminescence Counter; Perkin Elmer).

In Vivo Imaging

In vivo luciferase expression was analyzed 21 days after the injection with AAV9-Luc. Rats were anesthetized with 4% of isofluorane and placed in the imaging chamber of a Xenogen IVIS system (Xenogen, Alameda, CA, USA); anesthesia was maintained throughout the procedure. Rats were injected via the tail vein with 150 mg Luciferin/kg body weight (cat. no.: LUCK-100; Gold Biotechnology). A picture of the animals was taken, followed by bioluminescence image acquisition. Light intensity was quantified as photons/seconds/cm^2/sr. The color scale was normalized for all sets of images acquired.

ELISA

ELISA plates (cat. no.: 44-2404-21, Nunc MaxiSorp flat-bottom, Invitrogen) were coated with 1×10^{10} WT-AAV9 viral particles per well, overnight at 4°C. The WT-AAV9-coated plates were washed with 300 μL of PBS buffer per well and blocked with 300 μL of 5% non-fat milk in PBS for 1 h. In a separate 96-well plate, 2-fold serial dilutions of the sera, IVIG, or eluate solutions in 10% milk TBS-Tween (Tris Buffer Saline Tween) (Tris hydrochloride, 20 mM; NaCl, 150 mM, and Tween 20, 0.1%) were prepared and then incubated in the ELISA plate for 1 h at room temperature. After the incubation, the plate was washed 3 times with 300 μL of TBST (0.05%, v/v) per well and incubated for 1 h with goat anti-rat IgG-horseradish peroxidase (HRP) H&L (cat. no.: ab97057, Abcam; 1:10,000 in 5% fat-free milk in TBS-Tween) or rabbit anti-human IgG-HRP H&L (cat. no.: ab6759, Abcam; 1:10,000 in 5% fat-free milk in TBT-Tween). After washing each well 3 times with 300 μL of TBST the plate was incubated with HRP substrate SIGMAFAST OPD (P9187, Sigma-Aldrich) for 10 min followed by the addition of HCl 3 M to stop the reaction. The plate was read at 492 nm on a multiwell plate reader (Molecular Devices, SpectraMax).

Western Blot

1×10^9 AAV9 or AAV2 viral particles were mixed with sample buffer (62.5 mM Tris hydrochloride, pH 6.8, 10% v/v glycerol, 2% SDS, 1 mM DTT, and 0.005% bromophenol blue), heated at 95°C for 5 min and then loaded onto a 12% SDS-PAGE gels. After the electrophoresis, the proteins were transferred onto Immobilon-FL Transfer Membranes (cat. no.: IPFL00010; Millipore). The membranes were blocked with 5% fat-free milk in Tris-buffered saline (TBS) for 1 h at room temperature and incubated with the bead eluates as primary antibodies in blocking buffer overnight at 4°C (1:100 dilution). The membranes were washed three times in TBS-Tween (0.05%, v/v) and then incubated for 1 h at room temperature with (HRP)-conjugated secondary antibodies, either goat anti-rat IgG-HRP H&L (cat. no.: ab97057, Abcam) or rabbit anti-human IgG-HRP H&L (cat. no.: ab6759, Abcam; 1:1,000 in 5% fat-free milk in TBS-Tween). The membranes were then washed three times with TBS-Tween and the bands visualized using the Immobilon Western Chemiluminescence HRP Substrate (cat. no.: WBKLS0050, Millipore) and a ChemiDoc Imaging System (BioRad).

DNA Isolation and qPCR

Total DNA from rat blood was purified using a QIAGEN Blood and Tissue DNA extraction kit (QIAGEN, Hilden, Germany) according the manufacturer's instructions and eluted in 200 μL of elution buffer. Viral genome copy numbers were determined by quantitative polymerase chain reaction (qPCR) using primers that bind to the luciferase cDNA region: (fwd: 5′-ACAC CCGAGGGGGATGATAA-3′; rev: 5′-G TGTTCGTC TTCGTCCCAGT-3′). A standard curve was made by making serial dilutions of luciferase *cis*-plasmid in nuclease-free water. Dialyzed virus stocks were diluted 1:1,000 in nuclease-free water and qPCR mixtures were made up using the iTaq Universal SYBR Green Supermix (Bio-Rad Laboratories). The qPCR was carried out according to the manufacturer's instructions in a 7,500 Real-Time PCR System thermal cycler (Applied Biosystems) with the following thermal cycling parameters: one cycle of 95°C for 5 min followed by 40 cycles of 95°C for 10 s, 58°C for 10 s, and 72°C for 45 s.

Statistical Analysis

Statistical analysis was performed using version 7 of Prism for Mac (Graphpad). Analysis with the Shapiro-Wilk normality test demonstrated the absence of a normal distribution of luciferase expression in several groups. Therefore, group-to-group comparisons were performed using the Mann-Whitney test.

SUPPLEMENTAL INFORMATION

Supplemental Information can be found online at https://doi.org/10.1016/j.omtm.2020.01.004.

AUTHOR CONTRIBUTIONS

AO, MGK, SMG, TW designed and performed the experiments, ASF and KMF helped in the design of the experiments, AO and TW wrote the manuscript.

ACKNOWLEDGMENTS

This work was supported by NHLBI grant HL131404 (T.W.) and a Transatlantic Network of Excellence grant (14 CVD 03) by the Leducq Foundation (T.W.)

REFERENCES

1. Samulski, R.J., and Muzyczka, N. (2014). AAV-Mediated Gene Therapy for Research and Therapeutic Purposes. Annu. Rev. Virol. *1*, 427–451.
2. Clark, K.R., Sferra, T.J., and Johnson, P.R. (1997). Recombinant adeno-associated viral vectors mediate long-term transgene expression in muscle. Hum. Gene Ther. *8*, 659–669.
3. Keeler, A.M., and Flotte, T.R. (2019). Recombinant Adeno-Associated Virus Gene Therapy in Light of Luxturna (and Zolgensma and Glybera): Where Are We, and How Did We Get Here? Annu. Rev. Virol. *6*, 601–621.
4. George, L.A., Sullivan, S.K., Giermasz, A., Rasko, J.E.J., Samelson-Jones, B.J., Ducore, J., Cuker, A., Sullivan, L.M., Majumdar, S., Teitel, J., et al. (2017). Hemophilia B Gene Therapy with a High-Specific-Activity Factor IX Variant. N. Engl. J. Med. *377*, 2215–2227.
5. Rangarajan, S., Walsh, L., Lester, W., Perry, D., Madan, B., Laffan, M., Yu, H., Vettermann, C., Pierce, G.F., Wong, W.Y., and Pasi, K.J. (2017). AAV5-Factor VIII Gene Transfer in Severe Hemophilia A. N. Engl. J. Med. *377*, 2519–2530.
6. Boutin, S., Monteilhet, V., Veron, P., Leborgne, C., Benveniste, O., Montus, M.-F., and Masurier, C. (2010). Prevalence of serum IgG and neutralizing factors against adeno-associated virus (AAV) types 1, 2, 5, 6, 8, and 9 in the healthy population: implications for gene therapy using AAV vectors. Hum. Gene Ther. *21*, 704–712.
7. Calcedo, R., Vandenberghe, L.H., Gao, G., Lin, J., and Wilson, J.M. (2009). Worldwide epidemiology of neutralizing antibodies to adeno-associated viruses. J. Infect. Dis. *199*, 381–390.
8. Greenberg, B., Butler, J., Felker, G.M., Ponikowski, P., Voors, A.A., Pogoda, J.M., Provost, R., Guerrero, J., Hajjar, R.J., and Zsebo, K.M. (2016). Prevalence of AAV1 neutralizing antibodies and consequences for a clinical trial of gene transfer for advanced heart failure. Gene Ther. *23*, 313–319.
9. Monteilhet, V., Saheb, S., Boutin, S., Leborgne, C., Veron, P., Montus, M.F., Moullier, P., Benveniste, O., and Masurier, C. (2011). A 10 patient case report on the impact of plasmapheresis upon neutralizing factors against adeno-associated virus (AAV) types 1, 2, 6, and 8. Mol. Ther. *19*, 2084–2091.
10. Satyan, S., Alborzi, P., and Agarwal, R. (2006). Clinical Nephrology, Dialysis and Transplantation. Nat. Rev. Nephrol. *2*, E1, https://doi.org/10.1038/ncpneph0318.
11. Lazaridis, K., Dalianoudis, I., Baltatzidi, V., and Tzartos, S.J. (2017). Specific removal of autoantibodies by extracorporeal immunoadsorption ameliorates experimental autoimmune myasthenia gravis. J. Neuroimmunol. *312*, 24–30.
12. Lazaridis, K., Evaggelakou, P., Bentenidi, E., Sideri, A., Grapsa, E., and Tzartos, S.J. (2015). Specific adsorbents for myasthenia gravis autoantibodies using mutants of the muscle nicotinic acetylcholine receptor extracellular domains. J. Neuroimmunol. *278*, 19–25.
13. Makroo, R.N., Agrawal, S., Chowdhry, M., Kakkar, B., and Thakur, U.K. (2016). Efficacy of single, extended and goal directed immunoadsorption in ABO incompatible living related donor liver transplantation. Transfus. Apheresis Sci. *55*, 329–332.
14. Rostaing, L., Allal, A., Del Bello, A., Sallusto, F., Esposito, L., Doumerc, N., Debiol, B., Delas, A., Game, X., and Kamar, N. (2016). Treatment of large plasma volumes using specific immunoadsorption to desensitize ABO-incompatible kidney-transplant candidates. J. Nephropathol. *5*, 90–97.
15. Falese, L., Sandza, K., Yates, B., Triffault, S., Gangar, S., Long, B., Tsuruda, L., Carter, B., Vettermann, C., Zoog, S.J., and Fong, S. (2017). Strategy to detect pre-existing immunity to AAV gene therapy. Gene Ther. *24*, 768–778.
16. Majowicz, A., Nijmeijer, B., Lampen, M.H., Spronck, L., de Haan, M., Petry, H., van Deventer, S.J., Meyer, C., Tangelder, M., and Ferreira, V. (2019). Therapeutic hFIX Activity Achieved after Single AAV5-hFIX Treatment in Hemophilia B Patients and NHPs with Pre-existing Anti-AAV5 NABs. Mol. Ther. Methods Clin. Dev. *14*, 27–36.

17. Majowicz, A., Salas, D., Zabaleta, N., Rodríguez-Garcia, E., González-Aseguinolaza, G., Petry, H., and Ferreira, V. (2017). Successful Repeated Hepatic Gene Delivery in Mice and Non-human Primates Achieved by Sequential Administration of AAV5^{ch} and AAV1. Mol. Ther. *25*, 1831–1842.

18. Salas, D., Kwikkers, K.L., Zabaleta, N., Bazo, A., Petry, H., van Deventer, S.J., Aseguinolaza, G.G., and Ferreira, V. (2019). Immunoadsorption enables successful rAAV5-mediated repeated hepatic gene delivery in nonhuman primates. Blood Adv. *3*, 2632–2641.

19. Kotchey, N.M., Adachi, K., Zahid, M., Inagaki, K., Charan, R., Parker, R.S., and Nakai, H. (2011). A potential role of distinctively delayed blood clearance of recombinant adeno-associated virus serotype 9 in robust cardiac transduction. Mol. Ther. *19*, 1079–1089.

20. Huttner, N.A., Girod, A., Perabo, L., Edbauer, D., Kleinschmidt, J.A., Büning, H., and Hallek, M. (2003). Genetic modifications of the adeno-associated virus type 2 capsid reduce the affinity and the neutralizing effects of human serum antibodies. Gene Ther. *10*, 2139–2147.

21. Kwon, I., and Schaffer, D.V. (2008). Designer gene delivery vectors: molecular engineering and evolution of adeno-associated viral vectors for enhanced gene transfer. Pharm. Res. *25*, 489–499.

22. Mingozzi, F., Anguela, X.M., Pavani, G., Chen, Y., Davidson, R.J., Hui, D.J., Yazicioglu, M., Elkouby, L., Hinderer, C.J., Faella, A., et al. (2013). Overcoming preexisting humoral immunity to AAV using capsid decoys. Sci. Transl. Med. *5*, 194ra92.

23. Mingozzi, F., Chen, Y., Murphy, S.L., Edmonson, S.C., Tai, A., Price, S.D., Metzger, M.E., Zhou, S., Wright, J.F., Donahue, R.E., et al. (2012). Pharmacological modulation of humoral immunity in a nonhuman primate model of AAV gene transfer for hemophilia B. Mol. Ther. *20*, 1410–1416.

24. Sarin, H. (2010). Physiologic upper limits of pore size of different blood capillary types and another perspective on the dual pore theory of microvascular permeability. J. Angiogenes. Res. *2*, 14.

25. Hudlická, O. (1982). Growth of capillaries in skeletal and cardiac muscle. Circ. Res. *50*, 451–461.